SI Appendix

Coupling between D-3-phosphoglycerate dehydrogenase and D-2-hydroxyglutarate dehydrogenase drives bacterial L-serine synthesis

Wen Zhang[a,b], Manman Zhang[a], Chao Gao[a,1], Yipeng Zhang[a], Yongsheng Ge[a], Shiting Guo[a], Xiaoting Guo[a], Zikang Zhou[c], Qiuyuan Liu[a], Yingxin Zhang[a], Cuiqing Ma[a], Fei Tao[c], & Ping Xu[c,1]

[a]*State Key Laboratory of Microbial Technology, Shandong University, Jinan 250100, People's Republic of China*
[b]*Center for Gene and Immunotherapy*, *The Second Hospital of Shandong University, Jinan 250033, People's Republic of China*
[c]*State Key Laboratory of Microbial Metabolism, Shanghai Jiao Tong University, Shanghai 200240, People's Republic of China*

[1]Corresponding authors:

Mailing address for P. Xu: School of Life Sciences and Biotechnology, Shanghai Jiao Tong University, Shanghai 200240, People's Republic of China; Phone: +86-21-34206647, Fax: +86-21-34206723, E-mail: pingxu@sjtu.edu.cn
Mailing address for C. Gao: State Key Laboratory of Microbial Technology, Shandong University, Jinan 250100, People's Republic of China; Phone: +86-531-88364003, Fax: +86-531-88369463, E-mail: jieerbu@sdu.edu.cn

Table S1 Reference sequences (RefSeq) of SerA and homologous D2HGDH in different organisms. The identities between the predicted D2HGDH sequences and the D2HGDH from *Homo sapiens* were also listed.

Organism	**RefSeq and length of SerA proteins**	**RefSeq and length of D2HGDH proteins**	**Identity**
Bacteria			
Corallococcus coralloides DSM 2259	YP_005372922.1 (398 aa)	YP_005372923.1 (467 aa)	39%
Myxococcus xanthus DK 1622	YP_634480.1 (417 aa)	YP_634481.1 (468 aa)	39%
Stenotrophomonas maltophilia K279a	YP_001971994.1 (440 aa)	YP_001971995.1 (462 aa)	37%
Xanthomonas campestris pv. vesicatoria str. 85-10	YP_363621.1 (440 aa)	YP_363622.1 (496 aa)	36%
Bdellovibrio bacteriovorus HD100	NP_969677.1 (401 aa)	NP_969675.1 (461 aa)	34%
Hahella chejuensis KCTC 2396	YP_432925.1 (436 aa)	YP_432926.1 (467 aa)	36%
Acinetobacter baumannii SDF	YP_001706018.1 (410 aa)	YP_001706019.1 (469 aa)	34%
Psychrobacter arcticus 273-4	YP_263672. (408 aa)	YP_263671.1 (480 aa)	33%
Alcanivorax borkumensis SK2	YP_691788.1 (409 aa)	YP_691787.1 (465 aa)	34%
Pseudomonas putida KT2440	NP_747256.1 (409 aa)	NP_747255.1 (455 aa)	38%
Pseudomonas aeruginosa PAOI	NP_249007.1 (409 aa)	NP_249008.1 (464 aa)	34%
Pseudomonas stutzeri A1501	YP_001170946.1 (410 aa)	YP_001170947.1 (464 aa)	35%
Acidovorax ebreus TPSY	ACM32271.1 (409 aa)	ACM32594.1 (489 aa)	39%
Acetobacter pasteurianus	AKR49191.1 (419 aa)	AKR48804.1 (478 aa)	36%
Leptospira interrogans serovar Lai str. 56601	NP_712092.1 (411 aa)	NP_713641.2 (474 aa)	36%
Escherichia coli str. K-12 substr. MG1655	NP_417388.1 (410 aa)	Unknown enzyme	Unknown
Yersinia pestis A1122	AJJ74524.1 (413 aa)	Unknown enzyme	Unknown
Klebsiella pneumoniae subsp. pneumoniae 1158	AJC02886.1 (410 aa)	Unknown enzyme	Unknown
Enterobacter cloacae subsp. dissolvens SDM	AFM61457.1 (410 aa)	Unknown enzyme	Unknown
Eukaryotic microorganisms			
Magnaporthe oryzae 70-15	XP_003709661.1 (472 aa)	XP_003717091.1(DLD2) (544 aa)	52%

Neurospora crassa OR74A	XP_955999.1 (466 aa)	XP_957332.1(DLD2) (551 aa)	53%
Aspergillus niger CBS 513.88	XP_001398464.2 (474 aa)	XP_001400196.1 (545 aa)	53%
Schizosaccharomyces pombe 972h-	NP_587837.1 (466 aa)	NP_595342.1 (526 aa)	48%
Candida albicans SC5314	(1) XP_716332.1 (463 aa); (2) XP_716394.1 (463 aa)	(1) XP_720128.1 (527 aa); (2) XP_719996.1 (527 aa)	51%; 51%
Saccharomyces cerevisiae S288c	(1) NP_011004.3 (469 aa); (2) NP_012191.1 (469 aa)	(1) NP_010103.1(DLD2) (530 aa); (2) NP_010843.1 (DLD3) (496 aa)	53%; 47%
Kluyveromyces lactis NRRL Y-1140	XP_452614.1 (470 aa)	XP_455341.1 (543 aa)	53%
Plants			
Arabidopsis thaliana	NP_564034.1 (PGDH, 624 aa) ; NP_195146.1 (EDA9, 603 aa); NP_566637.2 (3-PGDH, 588aa)	NP_568003.2 (559 aa)	56%
Zea mays	ACG30584.1 (590 aa)	XP_008651099.1 (562 aa)	57%
Oryza sativa Japonica Group	NP_001054094.1 (613 aa)	XP_015646835.1 (559 aa)	57%
Brachypodium distachyon	XP_003580703.1 (616 aa); XP_014753040.1 (618 aa)	XP_003561332.1 (621 aa)	56%
Animals			
Homo sapiens	NP_006614.2 (533 aa)	AAH36604.2 (521 aa)	100%
Bos taurus	NP_001030189.1 (533 aa)	NP_001069446.1 (544 aa)	78%
Rattus norvegicus	NP_113808.1 (533 aa)	NP_001100396.1 (528 aa)	79%
Gallus gallus	XP_422226.2 (525 aa)	XP_422664.3 (548 aa)	68%
Danio rerio	NP_955871.1 (527 aa)	NP_001074066.1 (533 aa)	69%
Drosophila melanogaster	NP_609496.1 (332 aa)	NP_569982.1 (533 aa)	49%
Caenorhabditis elegans	NP_496868.1 (322 aa)	NP_496465.1 (487 aa)	46%

Table S2 Binding parameters of coenzymes and substrates to SerA as determined by ITC.

Titration[*]	K_A (M^{-1})[†]	N (Sites)
To apoprotein of SerA (E)		
NADH→E	$(1.19 \pm 0.38) \times 10^7$	0.926 ± 0.0103
2-KG→E	Undetected	Undetected
2-KG→E (pre-incubated with 200 μM NADH) [‡]	$(2.34 \pm 0.50) \times 10^6$	2.43 ± 0.0238
2-KG→E (pre-incubated with 200 μM NAD^+)	Undetected	Undetected
NAD^+→E	$(7.83 \pm 1.18) \times 10^4$	0.641 ± 0.0753
D-3-PG→E	Undetected	Undetected
D-3-PG→E (pre-incubated with 200 μM NAD^+) [‡]	$(2.90 \pm 0.57) \times 10^4$	3.40 ± 0.2190
D-3-PG→E (pre-incubated with 200 μM NADH)	Undetected	Undetected
D-2-HG→E [§]	$(1.34 \pm 1.57) \times 10^4$	1.03×10^{-5}
D-2-HG→E (pre-incubated with 200 μM NAD^+)[‡]	$(3.47 \pm 0.59) \times 10^4$	0.229 ± 0.2080
D-2-HG→E (pre-incubated with 200 μM NADH)	Undetected	Undetected
NAD^+→E (pre-incubated with 200 μM NADH)	Undetected	Undetected
NADH→E (pre-incubated with 200 μM NAD^+)	$(7.90 \pm 0.25) \times 10^6$	0.803 ± 0.0111
To as-isolated SerA ($E^{\#}$)		
NADH→$E^{\#}$	$(1.58 \pm 0.56) \times 10^7$	0.240 ± 0.00972
NAD^+→$E^{\#}$	$(5.97 \pm 1.76) \times 10^4$	1.77×10^{-6}
KG→$E^{\#}$ [‡]	$(4.89 \pm 0.83) \times 10^5$	0.557 ± 0.0251
D-3-PG→$E^{\#}$	Undetected	Undetected

[*] The arrows mean the ligands (substrates or coenzymes) titrate to the enzyme of SerA (E or $E^{\#}$).
[†] K_A, equilibrium association constant; K_D, the equilibrium disassociation constant. $K_D = 1/K_A$.
[‡] The reaction proceeds during the titration.
[§] The very little binding of D-2-HG for apoenzyme without NAD^+ pre-incubation may be due to the little residual NAD^+ in apoenzyme.

Table S3 Growth test of *P. stutzeri* A1501 wide-type strain (A1501-WT) and A1501-Δ*d2hgdh* in different medium.*

Medium	Strain	μ_m (h^{-1})	Mb ($g \cdot DCW \cdot L^{-1}$)	Vs ($g \cdot L^{-1} \cdot h^{-1}$)	Mhg ($g \cdot L^{-1}$)	Yhg ($g \cdot g^{-1}$)
Glucose	A1501-WT	0.491 ± 0.022	1.805 ± 0.035	0.223 ± 0.003	Undetected	Undetected
	A1501-Δ*d2hgdh*	0.424 ± 0.013	1.355 ± 0.031	0.184 ± 0.013	0.425 ± 0.014	0.121 ± 0.004
Glycerol†	A1501-WT	0.343 ± 0.010	1.898 ± 0.015	0.182	Undetected	Undetected
	A1501-Δ*d2hgdh*	0.283 ± 0.021	1.601 ± 0.023	0.158	0.456 ± 0.016	0.111 ± 0.004
Pyr	A1501-WT	0.744 ± 0.004	1.235 ± 0.003	0.409 ± 0.002	Undetected	Undetected
	A1501-Δ*d2hgdh*	0.714 ± 0.014	0.972 ± 0.057	0.388 ± 0.001	0.245 ± 0.007	0.057 ± 0.002
Suc	A1501-WT	0.703 ± 0.096	1.345 ± 0.062	0.335 ± 0.003	Undetected	Undetected
	A1501-Δ*d2hgdh*	0.539 ± 0.090	0.608 ± 0.064	0.117 ± 0.003	0.164 ± 0.032	0.059 ± 0.010
2-KG	A1501-WT	0.782 ± 0.003	1.082 ± 0.016	0.364	Undetected	Undetected
	A1501-Δ*d2hgdh*	0.565 ± 0.039	0.950 ± 0.043	0.322	0.163 ± 0.013	0.040 ± 0.003
Glu	A1501-WT	0.470 ± 0.019	0.980 ± 0.052	0.136 ± 0.009	Undetected	Undetected
	A1501-Δ*d2hgdh*	0.274 ± 0.010	0.875 ± 0.038	0.110 ± 0.017	0.128 ± 0.005	0.048 ± 0.005
LB	A1501-WT	0.655 ± 0.015	1.548 ± 0.006	Not determined	Undetected	Not determined
	A1501-Δ*d2hgdh*	0.576 ± 0.036	1.395 ± 0.032	Not determined	0.172 ± 0.005	Not determined

* The initial glucose concentration is about 3.5 $g \cdot L^{-1}$. The initial concentration of other carbon sources is about 4 $g \cdot L^{-1}$. Pyr, pyruvic acid; Suc, succinic acid; 2-KG, 2-ketoglutaric acid; Glu, L-glutamic acid; μ_m, the maximum specific growth rate; Mb, the obtained maximum biomass; Vs, the average velocity of substance consumption; Mhg, the maximum concentration of D-2-HG; Yhg, D-2-HG yield. Values are the average ±SD (N=3). † 1 mM octoate was added to promote growth (1).

Table S4 The distribution of homologs of D2HGDH or SerA in bacteria. Coverage > 90%, E value < e^{-30}, identity > 30%.

Organism	D2HGDH homologs	SerA homologs	Coexistence
Proteobacteria	1360	1586	599
Actinobacteria	276	125	24
Acidobacteria	1	1	1
Bacteroidetes	35	50	14
Spirochaetes	16	17	14
Firmicute	359	35	7
Cyanobacteria	20	11	1
Aquificae	16	0	0
Chlorobi	0	3	0
Chloroflexi	6	0	0
Chlamydiae	0	1	0
Deferribacteres	1	0	0
Deinococcus-Thermus	19	0	0
Dictyoglomi	0	1	0
Fibrobacteres	0	2	0
Fusobacteria	12	0	0
Nitrospirae	1	0	0
Ignavibacteriae	1	1	0
Synergistetes	2	0	0
Thermobaculum	1	0	0
Thermodesulfobacteria	4	0	0
Verrucomicrobia	4	0	0
Thermotogae	6	0	0
Tenericutes	2	0	0
Candidate division NC10	1	0	0
Total	2143	1833	660

Table S5 The Gibbs free energy of the reaction of D-3-PG oxidation in the real cell environment.

Substrate	*E. coli* (2)	MDA-MB-468 (3)	BT-20 (3)
D-3-PG	1500 μM	180 μM	110 μM
NAD^+	2600 μM	990 μM	770 μM
3PHP	Estimated 3 μM	Estimated 10 μM	Estimated 10 μM
NADH	83 μM	370 μM	186 μM
2-KG	440 μM	550 μM	470 μM
D-2-HG	Estimated below 50 μM *	93 μM	35 μM
ΔG (D-3-PG+NAD^+→3PHP+NADH) †	+8.0 $kJ \cdot mol^{-1}$	+23.0 $kJ \cdot mol^{-1}$	+23.1 $kJ \cdot mol^{-1}$
ΔG (D-3-PG+2-KG→3PHP+ D-2-HG) †	Below −17.2 $kJ \cdot mol^{-1}$	−7.6 $kJ \cdot mol^{-1}$	−8.4 $kJ \cdot mol^{-1}$

* The value was estimated according to intracellular D-2-HG concentrations in *P. stutzeri* A1501 in this study.

† ΔG of the reaction of D-3-PG oxidation in the real cell environment has been assessed according to the intracellular concentrations of product and reactant on the basis of the fundamental equation, where R is the gas constant, T is temperature in Kelvin, Q is the ratio of the product to reactant concentrations: $\Delta G = \Delta G^{\circ\prime}_{obs} + RT\ln Q$. $\Delta G^{\circ\prime}_{obs}$ can be used from Fig. 4A.

Table S6 Primers, plasmids and strains used in this study.

Strain, plasmid, or primer	Characteristics
Strain	
A1501-WT	wild strain of *P. stutzeri* A1501
A1501-pk18-*d2hgdh'*	*P. stutzeri* A1501 strain harboring chromosomal integration with pk18-*d2hgdh'* plasmid; Km^{r} *
A1501-pk18-*etf'*	*P. stutzeri* A1501 strain harboring chromosomal integration with pk18-*etf'* plasmid; Km^{r} *
A1501-Δ*d2hgdh*	*P. stutzeri* A1501 strain mutant obtained by exchanging the *d2hgdh* gene with the *d2hgdh'*
A1501-Δ*d2hgdh*-pk18-*serA'*	A1501-Δ*d2hgdh* strain harboring chromosomal integration with pk18*mobsacB*-*serA'* plasmid; Km^{r} *
A1501-Δ*etf*	*P. stutzeri* A1501 strain mutant obtained by exchanging the *etf* gene with the *etf'*
A1501-Δ*d2hgdh*Δ*serA*	A1501-Δ*d2hgdh* mutant obtained by exchanging the *serA* gene with the *serA'*
A1501-*d2hgdh*$^{+}$	A1501-Δ*d2hgdh* strain harboring the plasmid pBBR1MCS-5-*d2hgdh*; Gm^{r} *
A1501-*etf*$^{+}$	A1501-Δ*etf* strain harboring the plasmid pBBR1MCS-5-*etf*; Gm^{r} *
PAO1-WT	wild strain of *P. aeruginosa* PAO1
PAO1- pk18-*PA0317'*	*P. aeruginosa* PAO1 strain harboring chromosomal integration with pk18-*PA0317'* plasmid; Km^{r} *
PAO1-Δ*PA0317*	*P. aeruginosa* PAO1 strain mutant obtained by exchanging the *PA0317* gene with the *PA0317'*
BL-D2HGDH	*E. coli* BL21(DE3) strain harboring the expression plasmid pET-*d2hgdh*
BL-ETF	*E. coli* BL21(DE3) strain harboring the expression plasmid pET-*etfAB*
BL-ETFQO	*E. coli* BL21(DE3) strain harboring the expression plasmid pET-*etfqo*
BL-SerA	*E. coli* BL21(DE3) strain harboring the expression plasmid PET-*serA*
BL-SerC	*E. coli* BL21(DE3) strain harboring the expression plasmid PET-*serC*
BL-D2HGDH (without His-tag)	*E. coli* BL21(DE3) strain harboring the expression plasmid pET-*d2hgdh* (no tag)
Plasmid	

pk18*mobsacB*	Allelic exchange suicide vector mobilized by *E. coli* S17-1λ*pir*; for selecting double crossover; Km^rSuc^s *
pk18-*d2hgdh'*	pK18*mobsacB* carrying *d2hgdh'*
pk18-*etf'*	pK18*mobsacB* carrying *etfAB'*
pk18-*serA'*	pK18*mobsacB* carrying *serA'*
pk18-*PA0317'*	pK18*mobsacB* carrying *PA0317'*
pETDuet-1	vector for protein expression, Ap^r *
pET-*d2hgdh*	pETDuet-1 carrying *d2hgdh* gene
pET-*etfAB*	pETDuet-1 carrying *etfAB* gene
pET-*etfqo*	pETDuet-1 carrying *etfqo* gene
PET-*serA*	pETDuet-1 carrying *serA gene*
PET-*serC*	pETDuet-1 carrying *serC gene*
pET-*d2hgdh* (no tag)	pETDuet-1 carrying *d2hgdh* gene for expression of D2HGDH without His-tag
pBBR1MCS-5	broad host range cloning vector; Gm^r *
pBBR1MCS-5-*d2hgdh*	pBBR1MCS-5 carrying *d2hgdh* gene
pBBR1MCS-5-*etf*	pBBR1MCS-5 carrying *etfAB* gene
pRK2013	ColE1 ori, Km^r [a], *mob*, tra^+, helper plasmid for conjugation experiments
Primer	
PD1	5'- AATGGATCCGATGACCGACCCCGCCCTGAT - 3' †
PD2	5'- ATTAAGCTTTCAGGCCGCGAAGATCTTGC - 3' †
PE1	5'- AATGGATCCGATGAAGGTTCTTGTAGCTGTC - 3' †
PE2	5'- AATAAGCTTTCAGACGAGCCGTTCCAGCTCCG - 3' †
KE1	5'- AATGGATCCGATGAACCCCTTCTGCGAGATCG - 3' †
KE2	5'- AGCTCTTCGCCGACGAGCGCGACGGTCTGCAG - 3'
KE3	5'- CTGCAGACCGTCGCGCTCGTCGGCGAAGAGCT - 3'

CD1	5'- ATAGGTACCATGACCGACCCCGCCCTGAT - 3' †
CD2	5'-AATAAGCTTTCAGGCCGCGAAGATCTTG- 3' †
CE1	5'- ATAAAGCTTATGAAGGTTCTTGTAGCTGTC - 3' †
CE2	5'- AATGGATCCTCAGACGAGCCGTTCCAGCTCC - 3' †
PQO1	5'- ATAGGATCCGATGGAACGCGAATACATGGAA - 3' †
PQO2	5'- AATAAGCTTTTACATGTTGGGGTAGTTCGG - 3' †
PS1	5'- AATGGATCCGATGAGCCAGACCTCTCTCGA- 3' †
PS2	5'- AATAAGCTTTCAGAACAGCACGCGGCTGCG- 3' †
KS1	5'- GCGATCCAGGCCACGCAGAGGAAGCGTTCTTCTC- 3'
KS2	5'- GAGAAGAACGCTTCCTCTGCGTGGCCTGGATCGC- 3'
PSC1	5'- AATGGATCCGGTGGTCGGTAAAGAAACCAG- 3'
PSC2	5'- AATAAGCTTTCAGCCGTGCTCCTTCTCG- 3'
KPA1	5'- CCGGAATTCATGACCCGCGAAGCCCTGATC- 3' †
KPA2	5'- ACACCACCTCGAAGTCCTGGCAGACTACGGT- 3'
KPA3	5'- ACCGTAGTCTGCCAGGACTTCGAGGTGGTGT- 3'
KPA4	5'- CCCCCCGGGCTCTGCGTTGCGACACCTGCTACT- 3' †
ND1	5'- AATCATATGACCGACCCCGCCCTGATCGA- 3' †
ND2	5'- AATGATATCTCAGGCCGCGAAGATCTTGC- 3' †

* Km^r, Gm^r and Ap^r indicate resistance to kanamycin, gentamicin sulphate and ampicillin, respectively. Suc^s indicates sensitive to sucrose.

† *Hin*dIII, *Bam*HI, *Kpn*I, *Eco*RI, *Sma*I, *Nde*I and *Eco*RV restriction sites introduced in the primers are underlined.

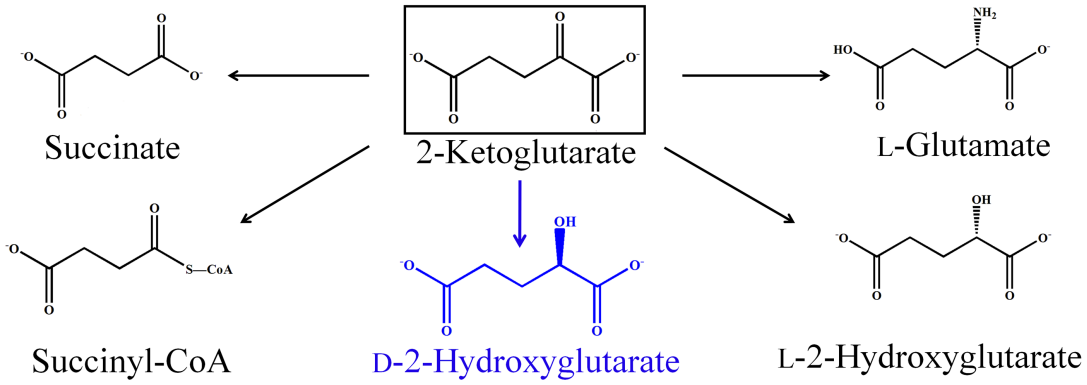

Fig. S1 The products generated from 2-KG in biochemical reactions.

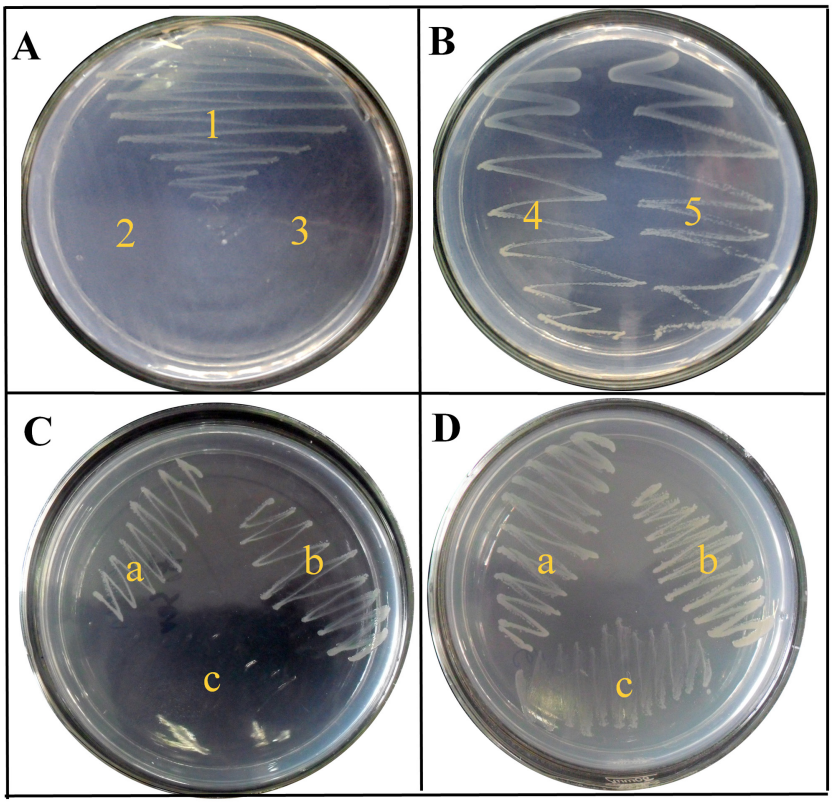

Fig. S2 The constructed strains with deletion or complementation of *d2hgdh*, *etf* or *serA*. Growth tests were performed on solid media supplemented with D-2-HG (A and B), glucose (C), or glucose plus 1 mM L-serine (D) as the sole carbon source. 1, A1501-WT; 2, A1501-Δ*d2hgdh*; 3, A1501-Δ*etf*; 4, A1501-Δ*d2hgdh-d2hgdh*$^{+}$; 5, A1501-Δ*etf-etf*$^{+}$; a, A1501-WT; b, A1501-Δ*d2hgdh*; c, A1501-Δ*d2hgdh*Δ*serA*.

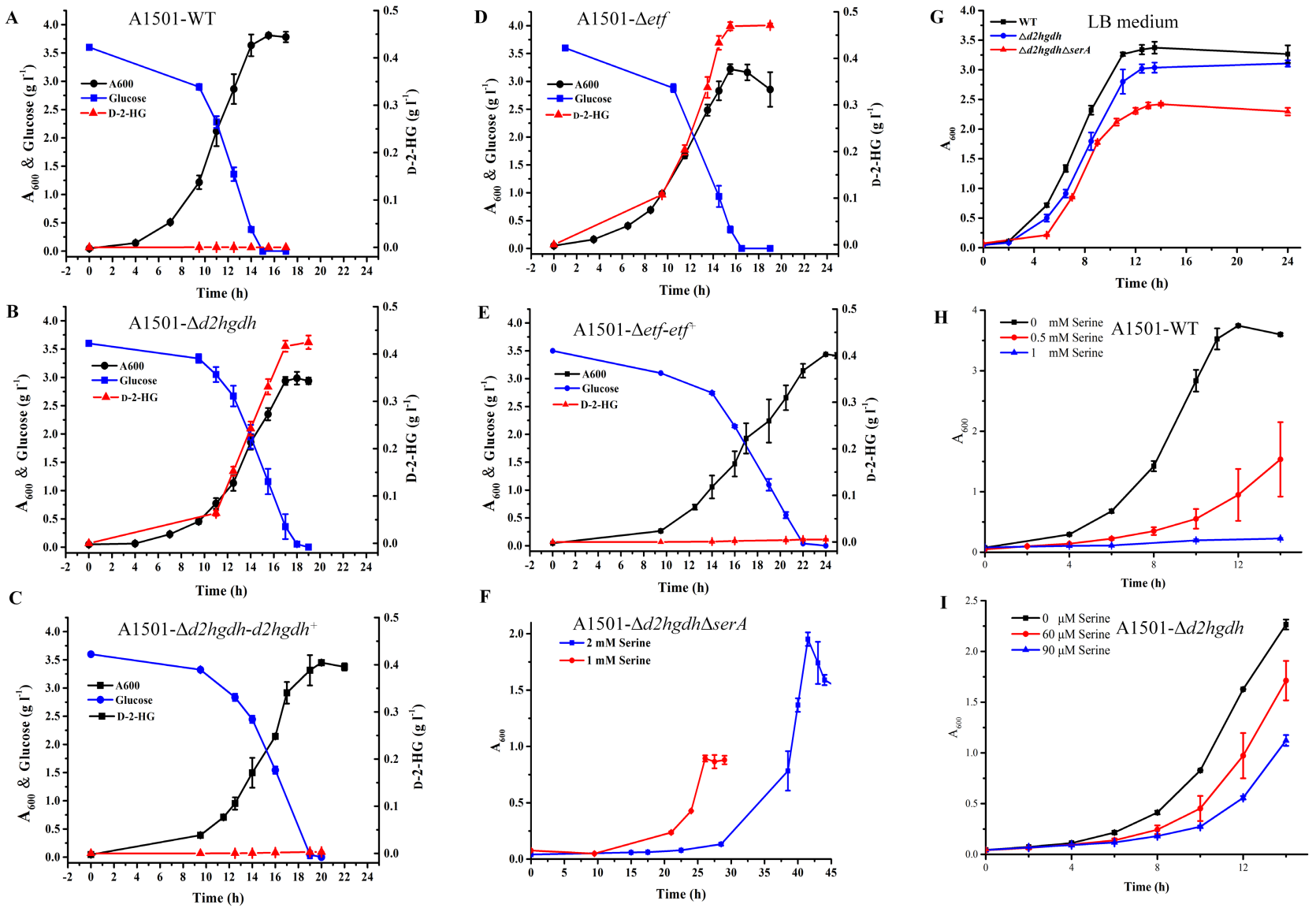

Fig. S3 Growth of *P. stutzeri* derivative strains in medium with glucose (3.5 g·L^{-1}) as sole carbon source (except G) or LB medium (G). Concentrations of D-2-HG and glucose in medium were determined in (A-E). L-Serine was added to the medium at corresponding concentrations in (F) (H) (I). Values are the average ±SD (N=3).

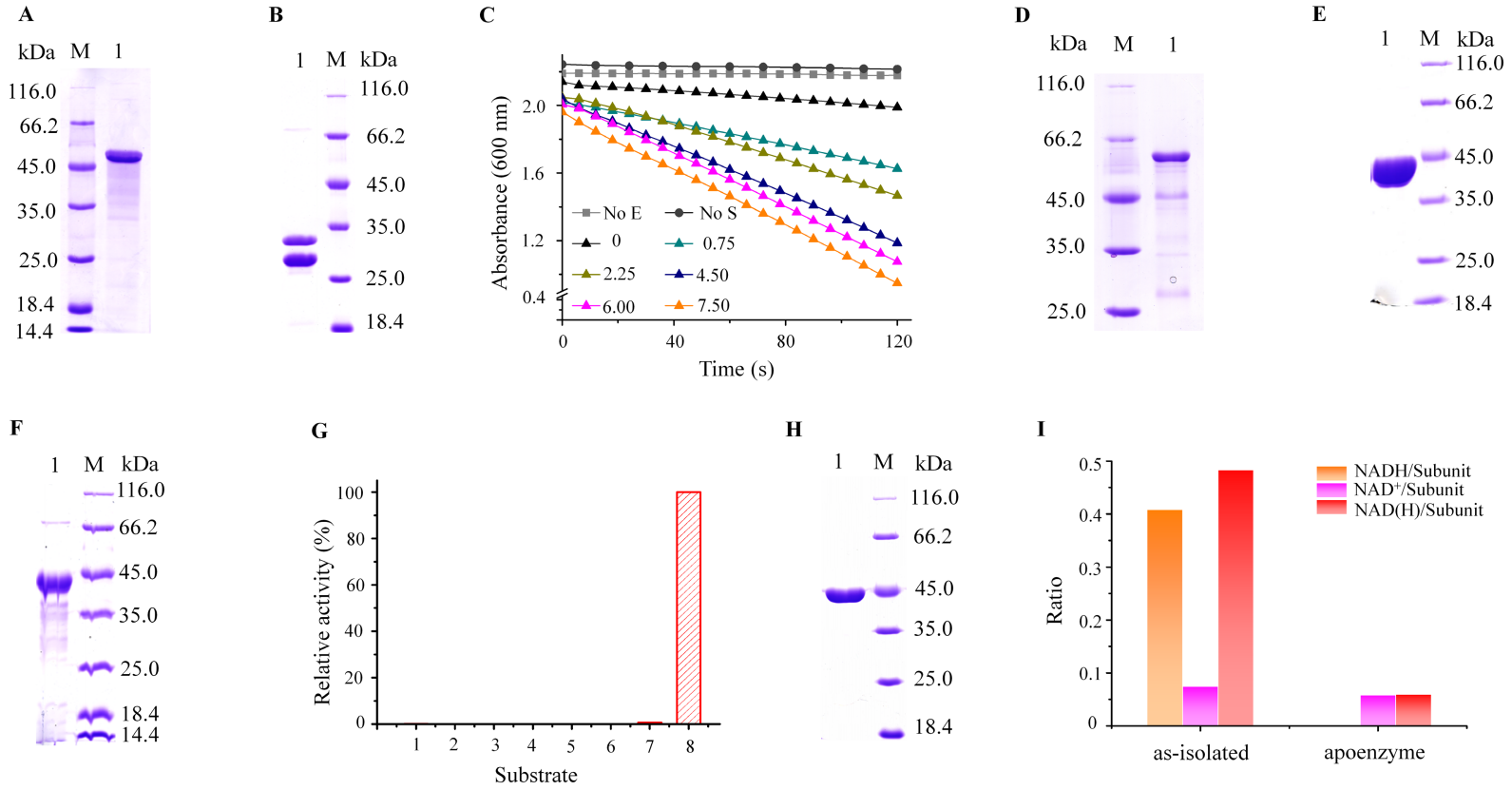

Fig. S4 The purified enzymes in this study and some of their properties. His-tagged D2HGDH (A), ETF (B), ETFQO (D), SerA (E) and SerC (H) that were cloned from *P. stutzeri* A1501, and His-tagged LGOR (F) that was cloned from *P. stutzeri* SDM for chiral analysis of 2-HG were analyzed by SDS-PAGE. Lane 1, the purified protein; lane M, Marker. (C) The effect of ETF (0–7.5 μM) on D2HGDH-catalyzed DCIP reduction in the presence of a fixed concentration of D-2-HG (0.5 mM). E, D2HGDH (0.14 μM); S, D-2-HG. (G) Substrate screening for LGOR. 1, L-lactate; 2, L-glycerate; 3, L-2-hydroxybutyrate; 4, glycollate; 5, DL-2-hydroxyoctanoate; 6, L-malate; 7, D-2-HG; 8, L-2-HG. Values are the average ±SD (N=3). (I) The ratio of the bound coenzyme to the subunit of SerA.

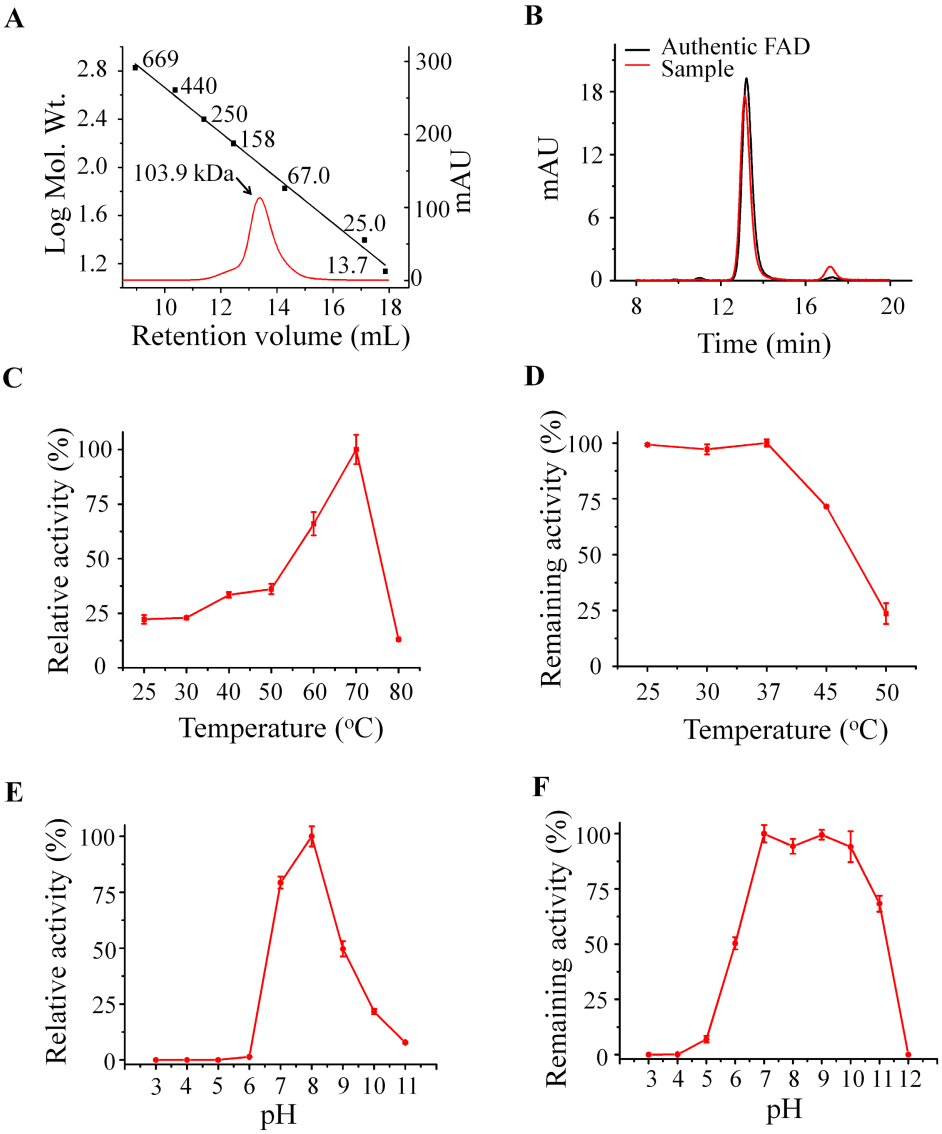

Fig. S5 Basic properties of the purified D2HGDH. (A) Size exclusion chromatography analysis of D2HGDH. Black line, standard curve for protein molecular mass standards; red curve, chromatogram of purified D2HGDH. (B) HPLC performance of authentic FAD (black line) and the released flavin (red line). Standard curve of FAD concentration related to peak area was obtained to determine the concentration of FAD released from D2HGDH and then the ratio between subunit of D2HGDH and FAD was calculated. (C) Effect of temperature on enzyme activity. The transient maximum activity was observed at 70 °C. (D) Effect of temperature on enzyme stability. The enzyme showed instability during incubation at temperatures higher than 37 °C. (E) Effect of pH on enzyme activity. The higher activities were determined at pH 7.0-8.0. (F) Effect of pH on enzyme stability. Little effect on the enzyme activity was observed after incubation at pH values ranging from 7.0 to 10.0 for one hour. Values are the average ±SD (N=3).

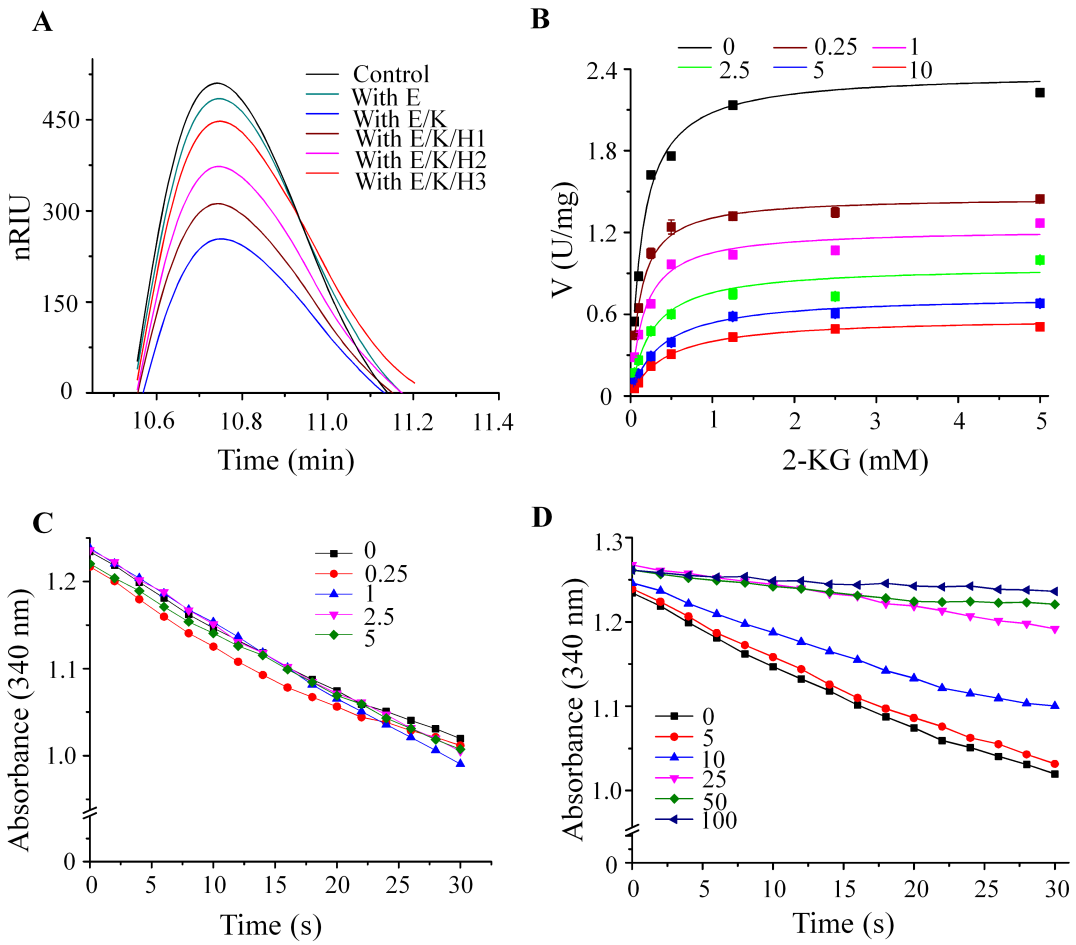

Fig. S6 Effects of D-2-HG, L-2-HG and L-serine on SerA function. (A) D-2-HG exhibits inhibitory effect on SerA. D-3-PG dehydrogenation catalyzed by SerA in the presence of 2-KG and D-2-HG was determined using HPLC by analyzing the peaks of residual D-3-PG present in the reaction mixtures (E, SerA; K, 2-KG; H1, 0.25 mM D-2-HG; H2, 1 mM D-2-HG; H3, 5 mM D-2-HG). The standard reaction mixtures containing SerA (1.3 μM), D-3-PG (1.25 mM), 2-KG (10 mM), and NAD^+ (2 mM) were incubated at 30 °C for 1.5 h. (B) Kinetic studies of SerA-catalyzed 2-KG reduction in the presence of various concentrations of D-2-HG (0–10 mM). As-isolated SerA, 0.36 μM; 2-KG, 0–5 mM; NADH, 200 μM. Values are the average ±SD (N=3). The data were fitted to a hyperbolic curve. (C) L-2-HG (0–5 mM) exhibits no inhibitory effect on the activities of SerA-catalyzed 2-KG reduction. (D) Addition of L-serine (0–100 μM) inhibits the reaction of SerA-catalyzed 2-KG reduction. The standard reaction mixtures for (C) and (D) contain 50 mM Tris (pH 7.4), 2-KG (2.5 mM), and NADH (200 μM).

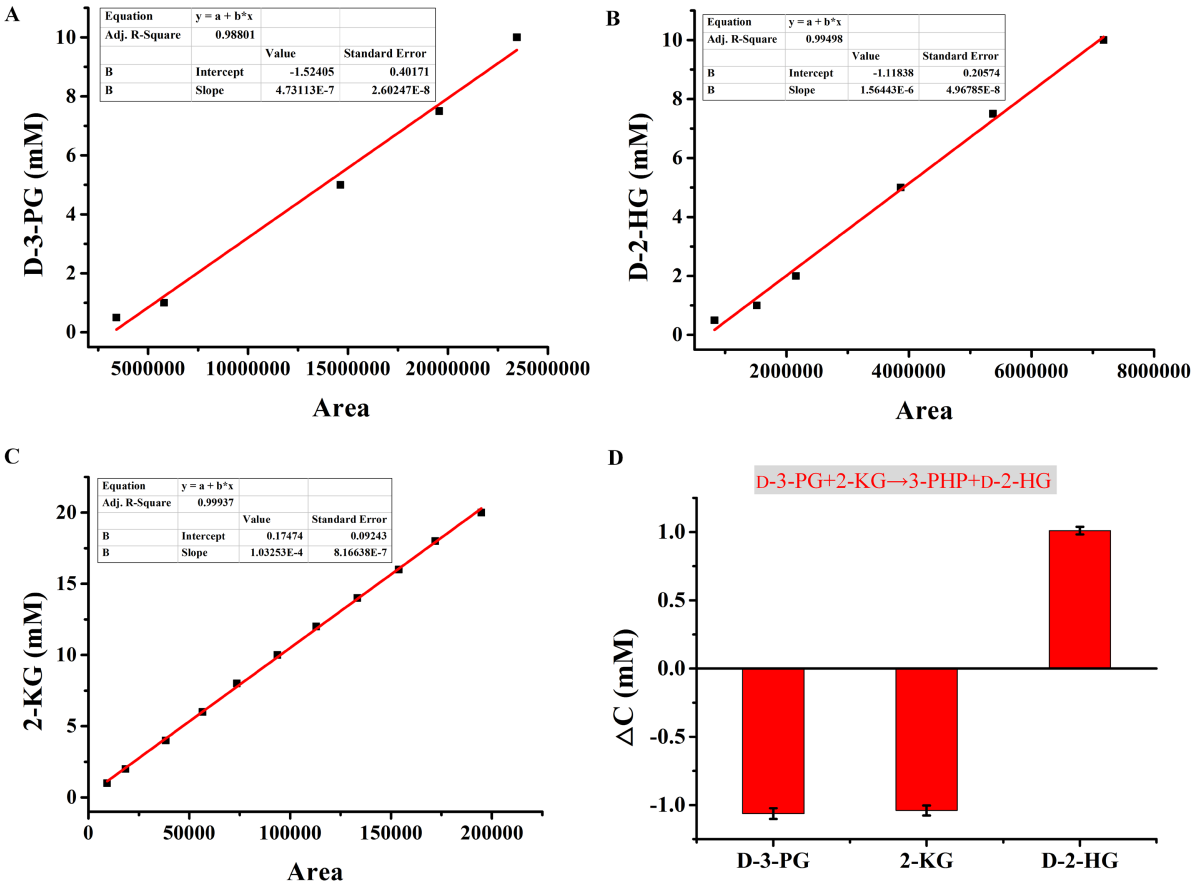

Fig. S7 Identification of the stoichiometry of the SerA-catalyzed coupled reaction. The standard curves of D-3-PG (A), D-2-HG (B) and 2-KG (C) were made by LC-MS (A and B) or HPLC (C). The reaction mixtures containing 50 mM Hepes (K^+) (pH 7.4), D-3-PG (5 mM), 2-KG (10 mM) and as-isolated SerA (13.9 μM) were incubated for 3 h at 30 °C, and then processed for quantification. The reaction mixture with heat-inactivated SerA was taken as a control. The changed concentrations (ΔC) of D-3-PG, 2-KG and D-2-HG after the reaction were shown in (D). The ratio of the consumption of D-3-PG (1.06 ± 0.04 mM) and 2-KG (1.04 ± 0.04 mM), and the increase of D-2-HG (1.01 ± 0.03 mM) is nearly 1:1:1 (D). Since the D-3-PG can only be converted into 3-PHP under the reaction conditions, the result mentioned above can demonstrate the equimolar conversion of D-3-PG and 2-KG to 3-PHP and D-2-HG.

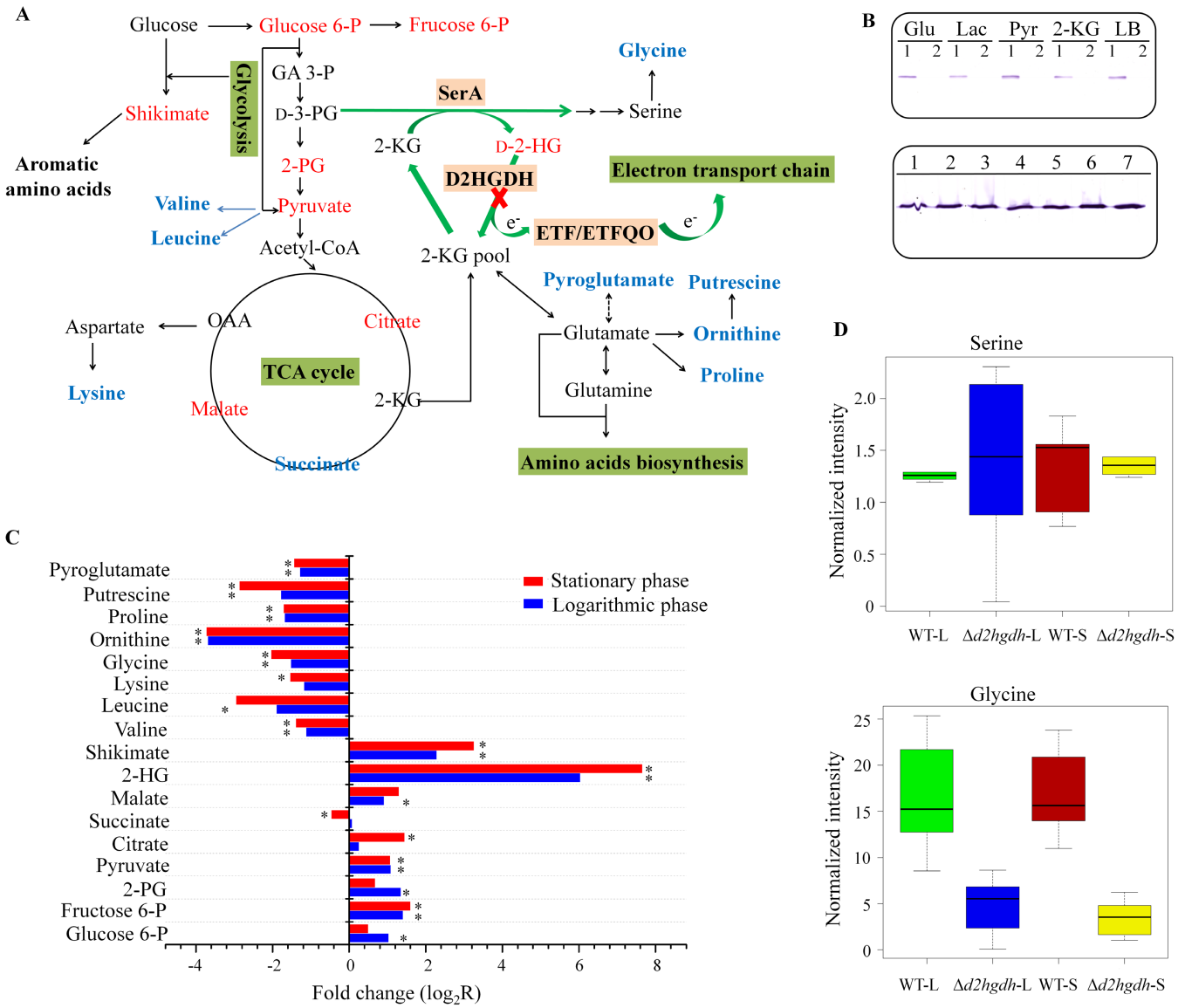

Fig. S8 HG-KG interconversion sits in the hub of central metabolism. (A) The HG-KG interconversion in the metabolic network drives L-serine biosynthesis and connects the core metabolism of glycolysis, TCA cycle, amino acid synthesis and electron transport chain in *P. stutzeri* A1501. According to Fig. S8C, the metabolites with higher levels as a result of D2HGDH knockout are shown in red color, while the metabolites with lower levels are shown in blue color. (B) D2HGDH activities in crude cell extracts of A1501-WT (number 1) and A1501-Δ*d2hgdh* (number 2) grown in LB or mediums with glucose (Glu), DL-lactate (Lac), pyruvate (Pyr) and 2-KG as the sole carbon source were determined by native PAGE and activity staining (the upper figure). D2HGDH activities in crude cell extracts of A1501-WT cells with glucose as the sole carbon source at different OD_{600} values (lanes 1–7: OD_{600} = 0.54, 1.16, 1.93, 2.25, 2.70, 3.24, and 3.56, respectively) with complete coverage of growth periods were also determined (the below figure). (C) The metabolites involved in the core metabolism with statistically change ($P<0.05$ and VIP>1, *) in at least one phase are identified due to the disruption of D2HGDH. VIP, the vip value of the first principal component in Partial Least Squares-Discriminant Analysis (PLS-DA). R represents the ratio of mean relative abundance of the metabolite in A1501-Δ*d2hgdh* group (N=6) and A1501-WT group (N=5). (D) The levels of serine and glycine within A1501-WT and A1501-Δ*d2hgdh* cells revealed by above metabolomic analysis. L, logarithmic phase; S, stationary phase.

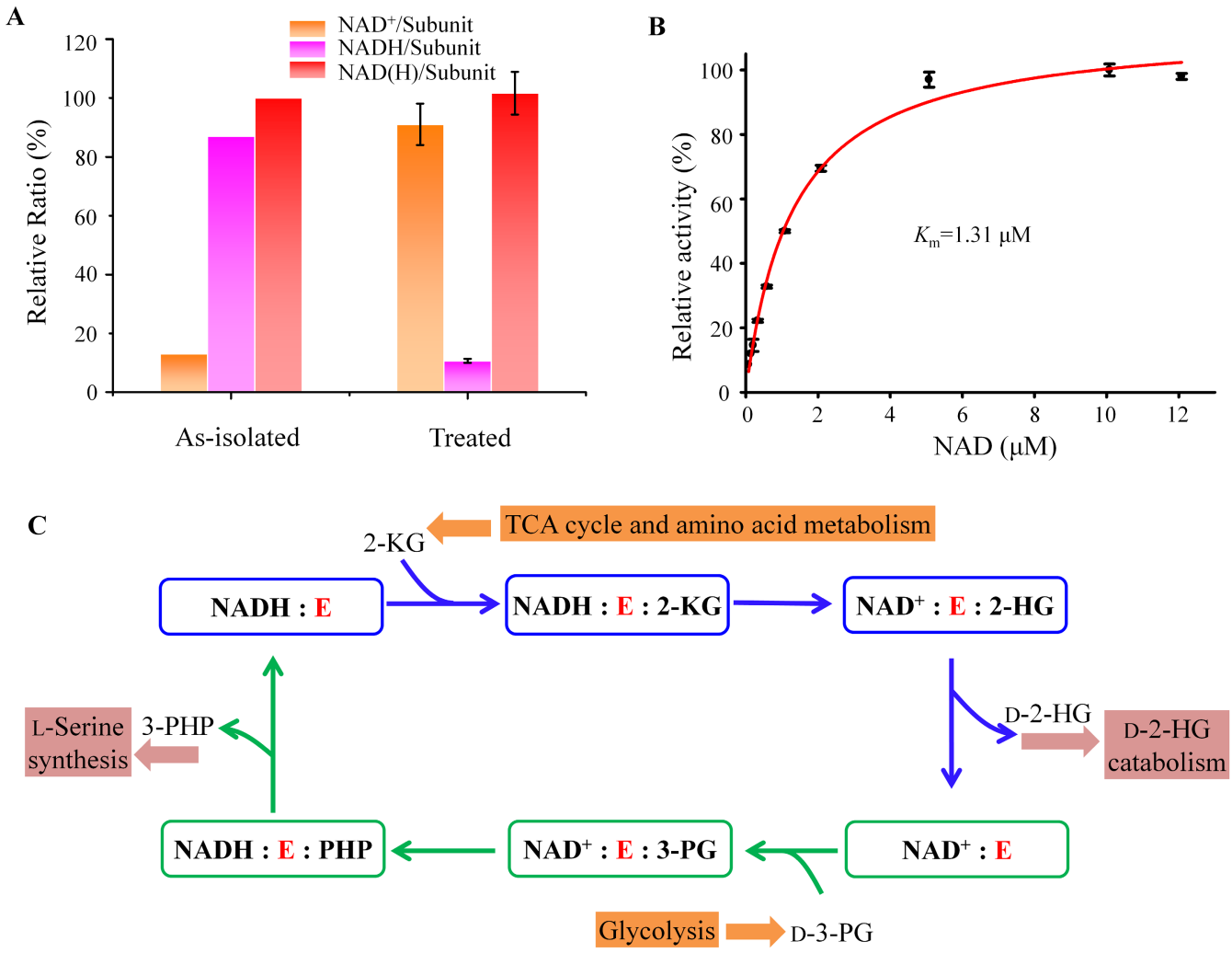

Fig. S9 NAD^+ and NADH seem to be not released during the enzymatic steps of the coupled reaction. (A) The relative ratio of coenzyme to the subunit. As-isolated SerA was firstly treated with 2-KG, and then pulled down by nickle-coupled agarose affinity matrix. The obtained SerA (Treated) and the as-isolated SerA were used to determine the bound NAD^+ and NADH. Values are the average ±SD (N=3) for treated SerA. (B) The apparent kinetics of the apoenzyme of SerA for NAD^+ without pre-incubation in the coupled reaction. The reaction mixtures containing 50 mM Hepes (K^+) (pH 7.4), 3-[(3-cholamidopropyl)dimethylammonio]-1-propanesulfonate (CHAPS, 6 mM), D2HGDH (1.2 μM), ETF (4.2 μM), CoQ_1 (53.2 μM), 2-KG (1 mM), D-3-PG (5 mM), ETFQO (1.6 μM) and as-isolated SerA (0.33 μM) were monitored by CoQ_1 reduction at 275 nm. Values are the average ±SD (N=2). (C) The proposed enzymatic steps for the coupled reaction catalyzed by SerA.

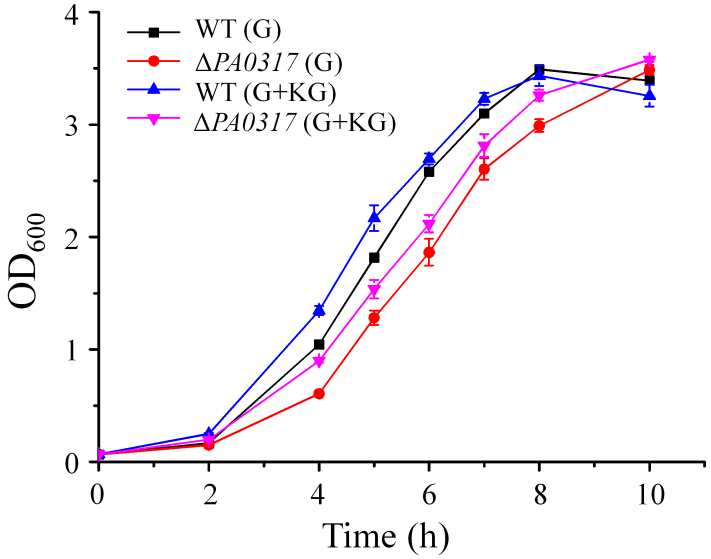

Fig. S10 Growth curves of different *P. aeruginosa* strains in the medium containing glucose (G) or glucose plus 2 mM 2-KG (G+KG). WT, the wild-type *P. aeruginosa* PAO1 strain; Δ*PA0317*, *P. aeruginosa* PAO1 strain with knockout of D2HGDH-encoding gene *PA0317*. Values are the average ± SD (N=3).

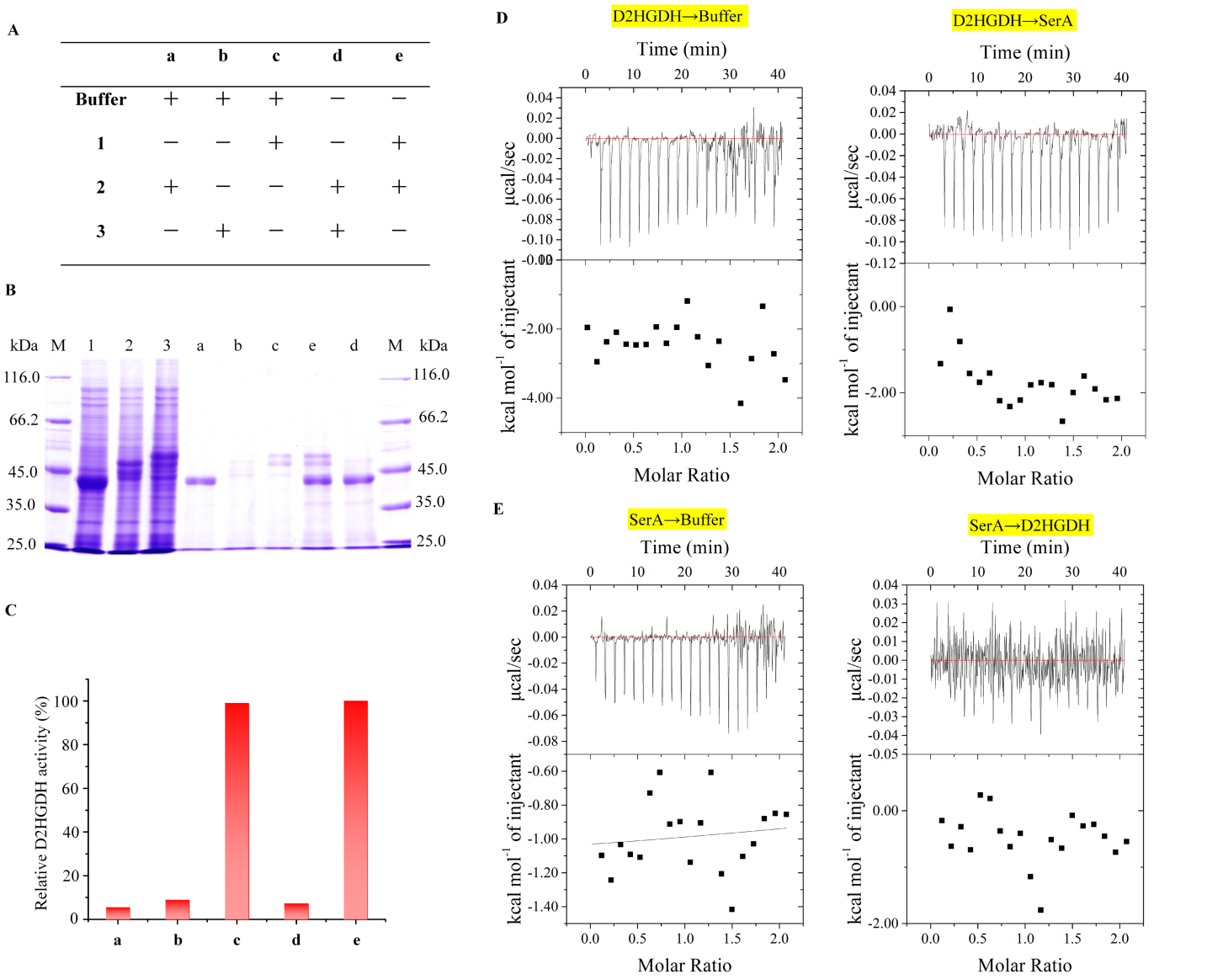

Fig. S11 Identification of the possible physical association between SerA and D2HGDH. (A) Design for the protein pull-down experiments. SerA with His-tag, D2HGDH with His-tag, and D2HGDH without His-tag were expressed, and the corresponding crude extracts were prepared. The pull-down experiments (a−e) were performed using nickle-coupled agarose affinity matrix with the corresponding crude extracts (mixed with the ratio of 1:1). Buffer, 50 mM Tris-HCl (pH 7.4); 1, the crude extracts of D2HGDH (with His-tag) expressing cells; 2, the crude extracts of SerA (with His-tag) expressing cells; 3, the crude extracts of D2HGDH (without His-tag) expressing cells. SDS-PAGE analysis (B) and D2HGDH activity assays (C) of the obtained proteins from the pull-down experiments. Lane 1−3, the crude extracts as above; Lane a−e, the obtained proteins. Compared group b with d, it is revealed that D2HGDH without His-tag could not be pulled down by SerA with His-tag. (D) D2HGDH (250 µM) titration to buffer or SerA (25 µM) by ITC. (E) SerA (250 µM) titration to buffer or D2HGDH (25 µM) by ITC. No apparent binding event was detected between D2HGDH and SerA, which further supports that there is no physical association between SerA and D2HGDH.

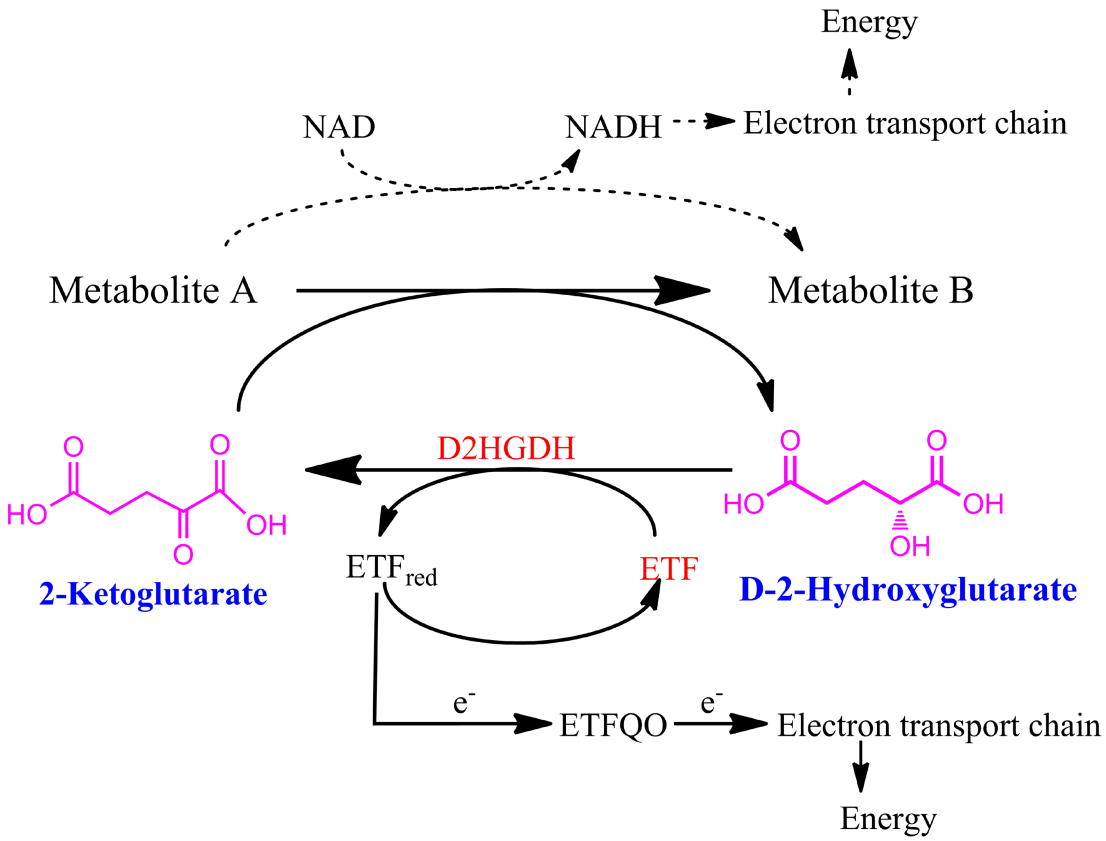

Fig. S12 The HG-KG interconversion represents a biochemical mechanism to drive unfavorable reactions for metabolite conversion (metabolite A to B), and meanwhile to realize electron transfer and energy production. ETF_{red}, reduced ETF.

Materials and Methods

Materials

Glycolic acid, D-lactate, D-glycerate calcium salt dihydrate, D,L-2-hydroxybutyrate, D,L-2-hydroxyglutarate disodium salt, D-mandelate, D-phenyllactic acid, D,L-2-hydroxyisocaproic acid, flavin adenine dinucleotide, cytochrome *c* from equine heart, 2-ketoglutarate, D-3-phosphoglycerate disodium salt, Coenzyme Q_1, NAD, NADH, resazurin, and hydroxypyruvic acid phosphate lithium salt were obtained from Sigma-Aldrich Co. LLC. (U.S.). Yeast extract powder and tryptone were obtained from Oxoid Limited (United Kingdom). Other chemicals were of analytical reagent grade.

Media and culture conditions

The minimum medium (adjusted to pH 7.0) for *Pseudomonas* was supplemented with NH_4Cl (0.1%) and different carbon sources as described previously (4). Cells were usually incubated aerobically at 30 °C (*P. stutzeri* A1501) or 37 °C (*P. aeruginosa* PAO1), with shaking at 200 rpm, and the cell density (OD_{600}) of the cultures was measured at various time points. Agarose (1.5%) was added to obtain solid medium. *E. coli* strains were grown in lysogenic broth (LB) medium at 37 °C. Antibiotics, such as ampicillin (100 $\mu g \cdot mL^{-1}$), gentamicin sulfate (40 $\mu g \cdot mL^{-1}$), kanamycin (50 $\mu g \cdot mL^{-1}$), and isopropyl β-D-thiogalactoside (IPTG; 1 mM) were used when necessary.

Enzyme preparation

ETF is a heterodimer (5). To express ETF accurately, the *etfA* gene (Gene ID: 5095566) and *etfB* gene (Gene ID: 5095567) from *P. stutzeri* A1501 were used. To express SerA, SerC and ETFQO, *serA* (Gene ID: 5094893), *serC* (Gene ID: 5098422) and *etfqo* (Gene ID: 25042155)

from *P. stutzeri* A1501 were used, respectively.

The plasmids and primers used in this study are listed in Table S6. The neighboring genes *etfA* and *etfB* from *P. stutzeri* A1501 were amplified as a whole by PCR with primers PE1 and PE2 and cloned into plasmid pETDuet-1 at the *Bam*HI and *Hin*dIII sites, resulting in pET-*etfAB* that overexpressed ETF with a hexahistidine tag fused to its N terminus. pET-*d2hgdh*, pET-*etfqo*, pET-*serA* and pET-*serC* plasmids were created as described above using primers PD1/PD2, PQO1/PQO2, PS1/PS2, and PSC1/PSC2, respectively. The obtained plasmids were transformed into BL21 (DE3) cells.

The constructed strains were grown in LB medium (100 μg·mL^{-1} ampicillin) at 37 °C to an optical density of 0.5–0.7 at 600 nm. Then IPTG was added at a final concentration of 1 mM, and the cells were grown at 16-30 °C overnight to induce expression. Cells were harvested by centrifugation at 13,000 × *g* for 7 min at 4 °C and suspended in binding buffer (pH 7.4, 20 mM sodium phosphate, 20 mM imidazole, 500 mM NaCl, 1 mM PMSF, and 10% glycerol). Cells were broken by ultrasonication as described previously (6) and centrifuged at 14,000 × *g* for 40 min at 4 °C. The supernatant (the crude extract) was loaded onto a 5 mL HisTrap HP column (GE Healthcare Life Sciences) equilibrated with binding buffer (20 mM sodium phosphate, 20 mM imidazole, 500 mM NaCl, pH 7.4), washed with 10% elution buffer (20 mM sodium phosphate, 500 mM imidazole, 500 mM NaCl, pH 7.4) to remove any weakly bound protein, and then eluted with different gradients of elution buffer at a flow rate of 5 mL·min^{-1}. For ETFQO overexpression, BL-ETFQO strain was grown in LB medium containing 2 μM riboflavin, 40 μM Fe^{3+} complexed with 8-hydroxyquinoline and 100 μg·mL^{-1} ampicillin (7). 1 mM IPTG was added to start induction when OD_{600} value reached 0.6–1.0. The cells were grown at 30 °C for 15 h and then harvested as above. The cell pellets were suspended in 50 mM Tris-HCl buffer (pH 7.4) containing n-octyl-β-D-glucopyranoside

(OG) and 0.1 mM DTT (7). The recombinant ETFQO was purified as above except 20 mM OG was added to the binding buffer and elution buffer. The obtained SerA without any treatment before purification was termed as as-isolated SerA. To obtain apoenzyme of SerA, sufficient amount of 2-KG (5–10 mM) was added to the cell suspensions before cell disruption, and 1 mM 2-KG was added to the binding buffer for complete reduction of NADH to NAD^+. After loading, it also required a wash step to remove the disassociated NAD^+ using 5–10 column volumes of this binding buffer. Then, this binding buffer was changed to the one without 2-KG for additional wash step to remove 2-KG. The other elution procedures remained the same. At last, the fractions containing target proteins were desalted with 50 mM Tris-HCl, Hepes (K^+) or sodium phosphate buffer (pH 7.4, containing 10% glycerol) using a 5 mL Hitrap Desalting column (GE Healthcare Life Sciences) and stored at −80 °C after concentration by ultrafiltration.

Molecular weight determination

A Superdex 200 10/300 GL column (GE Healthcare Life Sciences) used for size exclusion chromatography was equilibrated with wash buffer (50 mM sodium phosphate and 150 mM NaCl, pH 7.2) and calibrated with 0.8–1.0 mg each of five molecular mass standards (GE Healthcare Life Sciences) at a flow rate of 0.5 $ml \cdot min^{-1}$. The molecular mass of the protein was calculated from the standard curve based on the molecular masses of the protein standards.

Cofactor analysis for D2HGDH

The cofactor analysis procedure was performed as described previously (6) except that FAD was used instead of FMN. For the determination of the ratio between the recombinant

D2HGDH and FAD, 0.1143 mM of the recombinant D2HGDH was heated to 100 °C for 3 min and then centrifuged at 14,000 × g for 10 min to remove denatured protein. Cofactor released from purified protein was analyzed by HPLC. Standard FAD solutions of 0, 0.006, 0.015, 0.030, 0.060, 0.12 and 0.3 mM were used for quantitative analysis and detected at 450 nm. The concentration of the cofactor released from the recombinant D2HGDH was determined to be 0.2058 mM. Thus, the ratio between subunit of D2HGDH and FAD was (0.1143×2)/0.2058=1.11. Therefore, the native enzyme contains one FAD per subunit.

Coenzyme analysis for SerA

The coenzymes (NAD^+ or NADH) bound to SerA were extracted with methanol (8). Generally, the enzyme solutions (0.2–2 $mg \cdot ml^{-1}$) were treated with 9 volumes of methanol. After standing for 15 min on ice and a following centrifugation step (20,290 × *g* for 10 min at 0 °C), the precipipate was removed and the supernatant was evaporated at 30 °C. The residue was dissolved in appropriate volume of extraction buffer from NAD^+/NADH Quantification Kit (Biovision), and then NAD^+ and NADH were determined according to the protocol of the kit.

As-isolated SerA contains NADH, and 2-KG can oxidize NADH to NAD^+. Continuous dilution during purification process using Ni-chelating affinity chromatography causes release of NAD^+, which facilitates to obtain apoenzyme of SerA as above. To test whether the generated NAD^+ still binds to SerA in the real reaction mixtures, SerA (as-isolated; 10 μM) was firstly treated with 2-KG (1 mM) for 1 h. The protein was pulled down by nickle-coupled agarose affinity matrix (GE Healthcare Life Sciences) with the assistance of centrifugation step (14,000 × *g* for 5 min at 4 °C) instead of affinity chromatography. Then, after removal of the liquid as thoroughly as possible, the matrix was eluted by the elution

buffer to obtain the protein (called as treated SerA). The ratios of NAD^+ or NADH to subunit in as-isolated SerA or treated SerA were determined as above.

PAGE and activity staining

SDS-PAGE was performed using a 3.75% polyacrylamide stacking gel and an 11.25% polyacrylamide resolving gel, and Coomassie blue R-250 solution was used to visualize protein bands. For native-PAGE, SDS was omitted, and an ice-bath was used. Activity staining for D2HGDH was performed in 50 mM Tris-HCl buffer (pH 7.4) containing 400 μM phenazine methosulfate (PMS), 400 μM 3-(4,5-dimethylthiazol-2-yl)-2,5-diphenyltetrazolium bromide (MTT) and 1 mM D-2-HG.

Effect of pH and temperature on the activity and stability of D2HGDH

The 200 μl reaction mixtures containing 1 mM D-2-HG, 200 μM PMS, 200 μM DCIP and 0.2 μM purified D2HGDH were used to study the effect of pH and temperature on the activity and stability of D2HGDH. Enzyme suspension buffer and reaction buffer for temperature-related experiments was 50 mM Tris-HCl (pH 7.4). Enzyme suspension buffer for the study of pH effect on enzyme activity was 0.85% NaCl, while reaction buffers with a series of pH values were employed as described previously (6). For the study of pH effect on enzyme stability, the enzyme was diluted in above buffers with different pH values, and reacted in 50 mM Tris-HCl (pH 7.4). To study enzyme stability, the enzymes were incubated for 30 min or 60 min at the corresponding temperatures or pH, respectively, before the reaction. ε values of DCIP at different pH were calibrated as described (9).

Chromosomal deletion of targeted genes

A1501-Δ*d2hgdh*, A1501-Δ*etf*, A1501-Δ*d2hgdh*Δ*serA*, and PAO1-Δ*PA0317* mutant strains were obtained by disrupting the *d2hgdh*, *etfAB* and *serA* genes in *P. stutzeri* A1501, and *PA0317* (encodes D2HGDH) in *P. aeruginosa* PAO1, respectively, with the plasmid pk18*mobsacB* (Table S6). The plasmid pET-*d2hgdh,* which contains three *Eco*RI sites in the *d2hgdh* gene (296, 749, 842 bp), was digested with *Eco*RI*,* and the larger segment was purified and then circularized using T4 DNA ligase, resulting in a vector containing a disruption of *d2hgdh*, named *d2hgdh'* (849 bp). Two fragments, *etf1* and *etf2* were amplified by primers KE1/KE2 and KE3/PE2 and fused into *etfAB'* that is homologous to *etf* gene. The upstream fragment and downstream fragment of the *serA* gene were amplified and fused into *serA'* by primers PS1/KS1 and KS2/PS2. Similarly, the homologous fragment *PA0317'* was constructed using primers KPA1/KPA2 and KPA3/KPA4. *d2hgdh'*, *etfAB'*, *serA'* and *PA0317'* were then inserted into pk18*mobsacB*, a mobilizable plasmid that does not replicate in *Pseudomonas*, to form pk18-*d2hgdh'*, pk18-*etf'*, pk18-*serA'* and pk18-*PA0317'*, respectively. These resulted plasmids were transformed into *P. stutzeri* A1501 or *P. aeruginosa* PAO1 by the triparental mating method in the presence of the helper strain *E. coli* HB101 carrying pRK2013. The single crossover strains were isolated as previously described (6). The cells were first washed in 0.15 M NaCl and then screened on LB medium with 15% sucrose. The correct cells, called A1501-Δ*d2hgdh*, A1501-Δ*etf* and PAO1-Δ*PA0317* were identified and confirmed by PCR and a growth test. pk18-*serA'* was transformed into A1501-Δ*d2hgdh*, and the following operations were performed as above. The resulting double gene mutant strain was called A1501-Δ*d2hgdh*Δ*serA*.

Complementation of the targeted genes

To achieve complementation of the *P. stutzeri* A1501-*d2hgdh* and *etf* mutant, the *d2hgdh* and

etf genes were amplified by PCR using the primers CD1/CD2 and CE1/CE2, which contain *Kpn*I/*Hin*dIII and *Hin*dIII/*Bam*HI restriction enzyme sites. The PCR products were cloned into the vector pBBR1MCS-5, which carries the gentamicin resistance gene (10). The recombinant plasmid pBBR1MCS-5-*d2hgdh* or pBBR1MCS-5-*etf* was then introduced into A1501-Δ*d2hgdh* or A1501-Δ*etf* by triparental mating as above, except gentamicin sulfate was used instead of kanamycin. The resulting strains harboring the above plasmids were isolated as A1501-Δ*d2hgdh*-*d2hgdh*$^{+}$ or A1501-Δ*etf*-*etf*$^{+}$.

Modeling growth

The OD_{600} values at zero time and different time points were defined as A_0 and A, respectively. Growth curves obtained by plotting the logarithm of A/A_0 against time were fitted with the Gompertz model, and then the maximum specific growth rate (μ_m) was calculated (11).

Metabolome analysis

For sampling of intracellular metabolites, cells (300 mg) in middle-later logarithmic phase and stationary phase were quenched with two volumes of 60% methanol (−40 °C), centrifuged (4,000 × g, 4 °C, 10 min), washed with pre-cooled PBS (4 °C), and finally harvested by centrifugation (5,000 × g, 4 °C, 5 min). The cell pellets were suspended in 500 μL methanol (−20 °C) and 500 μL ddH_2O (4 °C), and then vortexed 30 seconds. After addition of 60 μL nonadecanoic acid (0.2 mg·mL^{-1}) as internal standard, glass beads (100 mg, Sigma glass beads G8772-100G) was added into the tubes for another vortex (1 min), and the freeze-thaw cycles were performed three times. The supernatants were obtained by centrifugation (13,000 × g, 4 °C, 10 min) and then dried. For derivatization, the residues were

dissolved in 60 μL methoxamine hydrochloride (15 mg·mL^{-1}), vortexed (30 s), and incubated at 37 °C for 2 h. 60 μL BSTFA (containing 1% trimethylchlorosilane) was added and the mixtures reacted at 37 °C for 90 min. In order to allow retention indices calculations, 1μL standards for n-alkanes (C8-C20, C21-C40, Fluka Chemika, Switzerland) were also introduced. Six biological replicates were performed.

A sample aliquot of 1 μL was injected (split ratio, 20:1) in Agilent 7890A/5975C equipped with a HP-5MS column (Agilent J&W scientific, Folsom, USA). The temperature for injector or ion source was 280 °C or 250 °C, respectively. The oven temperature started from 70 °C (2 min), increased to 300 °C (10°C per seconds), and then held for 5 min. The total run time was 30 min. The ionization energy (70 eV) was set and masses (35−780) were acquired. XCMS (www.bioconductor.org/) was used for data processing (12), and National Institute of Standards and Technology (NIST) database and Wiley Registry database were used for metabolite annotation, which can be further verified through comparing the retention indices with The Golm Metabolome Database (GMD) (http://gmd.mpimp-golm.mpg.de/) (13). For analysis of multivariate data, unsupervised Principal Component Analysis (PCA) using Simca-P 13.0 (Umetrics AB, Umea, Sweden) and supervised Partial Least Squares-Discriminant Analysis (PLS-DA) were performed. R version 3.0.3 (www.r-project.org) was used to perform Student's t test. The metabolites with statistic difference should meet $P<0.05$ and VIP (VIP value of the first component in PLS-DA) greater than 1.

Pull-down experiment

Firstly, to express D2HGDH without His-tag, *d2hgdh* gene was amplified using primers ND1/ND2 and cloned into *Nde*I/*Eco*RV sites of pETDuet-1. SerA with His-tag, D2HGDH

with His-tag, and D2HGDH without His-tag were expressed, and the crude extracts were prepared as above. The corresponding crude extracts (0.5 mL) were mixed (1:1) to form different groups (Fig. S11A). Then, nickle-coupled agarose affinity matrix (GE Healthcare Life Sciences) (0.25 mL) was added and mixed. After standing (10 min) and centrifugation (14,000 × *g* for 5 min at 4 °C), the matrix was washed with 50 mM Tris (pH 7.4) and another step of centrifugation was needed. The liquid should be removed as thoroughly as possible, and the elution buffer (0.5 mL) was used to elute the binding protein.

Isothermal titration calorimetry (ITC)

For the ITC experiments, SerA and other chemicals were freshly prepared in the same buffer containing 50 mM Tris-HCl buffer (pH 7.4) and 10% glycerol (v/v). Calorimetric assays were performed on an ITC200 (MicroCal, USA) in a 200 μl reaction cell loaded with 25 μM SerA (100 μM subunit) solutions at 25 °C. Titration was performed with an initial 0.4 μl injection of other chemicals in the syringe followed by 19 injections (2 μl) spaced by 120 s intervals. A control experiment was performed by titrating buffer into the SerA solution. The stirring speed was 1000 rpm and the reference power was 5 μcal s^{-1}. The net heat of the dilutions was corrected by subtracting the average heat of the control. The binding isotherms were fitted to a single site binding model using the Origin 7.0 software package supplied with the instrument, giving values for the stoichiometry (N) of binding and the equilibrium association constant (K_A).

Determination of the intracellular NAD^+ and NADH concentrations

NAD^+ and NADH were extracted separately. Three separate cell cultures of *P. stutzeri* A1501 were sampled (about 1–2 mL). After removal of the medium, the pellet was resuspended in

300 µl 0.2 M hydrochloric acid (HCL) for NAD^+ extraction or 0.2 M sodium hydroxide (NaOH) for NADH extraction, and incubated at 50 °C for 10 min. Then, 300 µl 0.1 M NaOH for NAD^+ extraction or 0.1 M HCL for NADH extraction was added and mixed rapidly. After centrifugation at 12,000 × g for 10 min, the supernatant was obtained for further determination by NAD^+/NADH Quantification Kit (Biovision). The standard curves for NAD^+ and NADH were also prepared separately: NAD^+ standard was dissolved in the solution (0.2 M NaOH : 0.1 M HCL = 1:1) while NADH standard was dissolved in the other solution (0.2 M HCL : 0.1 M NaOH= 1:1). We assumed that the cell volume of a 1-mL *Pseudomonas* sample at an optical density (600 nm) of 1 was 3.5 µL (14). Then, the intracellular volumes of the cells were estimated. We determined that the intracellular level of NAD^+ at mid-logarithmic phase was 107 µM and the value at stationary phase was 190 µM. For NADH, the values at mid-logarithmic phase and stationary phase were 137 µM and 170 µM, respectively.

References

1. Escapa IF, del Cerro C, Garcia JL, Prieto MA (2013) The role of GlpR repressor in *Pseudomonas putida* KT2440 growth and PHA production from glycerol. *Environ Microbiol* 15:93−110.
2. Bennett BD*, et al.* (2009) Absolute metabolite concentrations and implied enzyme active site occupancy in *Escherichia coli*. *Nat Chem Biol* 5:593−599.
3. Fan J*, et al.* (2015) Human phosphoglycerate dehydrogenase produces the oncometabolite D-2-hydroxyglutarate. *ACS Chem Biol* 10:510−516.
4. Baginsky ML, Rodwell VW (1966) Metabolism of pipecolic Acid in a *Pseudomonas* Species IV. Electron transport particle of *Pseudomonas putida*. *J Bacteriol* 92:424−432.
5. Toogood HS*, et al.* (2004) Extensive domain motion and electron transfer in the human electron transferring flavoprotein.medium chain Acyl-CoA dehydrogenase complex. *J Biol Chem*

279:32904−32912.

6. Gao C*, et al.* (2012) NAD-independent L-lactate dehydrogenase is required for L-lactate utilization in *Pseudomonas stutzeri* SDM. *PLoS One* 7:e36519.

7. Usselman RJ*, et al.* (2008) Impact of mutations on the midpoint potential of the [4Fe-4S]+1,+2 cluster and on catalytic activity in electron transfer flavoprotein-ubiquinone oxidoreductase (ETF-QO). *Biochemistry* 47:92−100.

8. Kato N, Yamagami T, Shimao M, Sakazawa C (1986) Formaldehyde dismutase, a novel NAD-binding oxidoreductase from *Pseudomonas putida* F61. *Eur J Biochem* 156:59−64.

9. Armstrong JM (1964) The molar extinction coefficient of 2,6-dichlorophenol indophenol. *Biochim Biophys Acta* 86:194−197.

10. Kovach ME*, et al.* (1995) Four new derivatives of the broad-host-range cloning vector pBBR1MCS, carrying different antibiotic-resistance cassettes. *Gene* 166:175−176.

11. Zwietering MH, Jongenburger I, Rombouts FM, van 't Riet K (1990) Modeling of the bacterial growth curve. *Appl Environ Microbiol* 56:1875−1881.

12. Smith CA, Want EJ, O'Maille G, Abagyan R, & Siuzdak G (2006) XCMS: processing mass spectrometry data for metabolite profiling using nonlinear peak alignment, matching, and identification. *Anal Chem* 78:779−787.

13. Kopka J*, et al.* (2005) GMD@CSB.DB: the Golm Metabolome Database. *Bioinformatics* 21:1635−1638.

14. Volkmer B, Heinemann M (2011) Condition-dependent cell volume and concentration of *Escherichia coli* to facilitate data conversion for systems biology modeling. *PLoS One* 6:e23126.